Vibronic Participation of the Bridging Ligand in Electron Transfer and Delocalization: New Application of a Three-State Model in Pyrazine-Bridged Mixed-Valence Complexes of Trinucl...

ARTICLE *in* THE JOURNAL OF PHYSICAL CHEMISTRY A · OCTOBER 2003

Impact Factor: 2.69 · DOI: 10.1021/jp035643q

2 AUTHORS:

Casey H. Londergan
Haverford College
28 PUBLICATIONS **632** CITATIONS
SEE PROFILE

Clifford P. Kubiak
University of California, San Diego
246 PUBLICATIONS **8,453** CITATIONS
SEE PROFILE

Vibronic Participation of the Bridging Ligand in Electron Transfer and Delocalization: New Application of a Three-State Model in Pyrazine-Bridged Mixed-Valence Complexes of Trinuclear Ruthenium Clusters

Casey H. Londergan and Clifford P. Kubiak*

Department of Chemistry and Biochemistry, University of California, San Diego, Department 0358, 9500 Gilman Drive, La Jolla, California 92093-0358

Received: June 10, 2003; In Final Form: August 27, 2003

The importance of the bridging ligand in mediating electronic communication and delocalization between charge centers in near-delocalized mixed-valence complexes is investigated in the specific context of pyrazine-bridged, hexanuclear ruthenium complexes that display electron-transfer rates on the order of $10^{11}-10^{12}$ s^{-1}, as observed by partial coalescence of infrared bands. It is shown that a three-state vibronic model explicitly including the electronic and vibrational participation of the bridging ligand is needed to account for infrared and resonance Raman evidence of vibronic activity in symmetric modes of the bridging pyrazine ligand. The specific molecular orbital and normal-mode basis for this application of the three-state model is presented using experimental observations and density functional calculations on model trinuclear ruthenium clusters. An important conclusion of the application of this model is that infrared activity of symmetric bridging ligand modes in mixed-valence complexes is not a reliable indicator of electronic asymmetry on the vibrational time scale. The three-state model is shown to qualitatively reproduce the "tunability" of electronic communication observed in these complexes. The central importance of such a direct consideration of the bridging ligand in similar near-delocalized or delocalized complexes (like the well-known Creutz−Taube ion) is re-emphasized in this study.

1. Introduction

1.1. Electron Transfer in Pyrazine-Bridged Ruthenium Mixed-Valence Clusters. Despite the wealth of experimental data for mixed-valence complexes displaying strong electronic communication between sites and spectral indications of near-delocalized behavior, electron transfer (ET) and delocalization in such complexes are still the subject of much recent discussion.[1] A mixed-valence system of recent investigation that has stimulated much discussion and some disagreement is the "dimer" of ruthenium trinuclear acetate clusters, $\{Ru_3O(OAc)_6(L)(CO)\}_2(\mu\text{-pz})^{1-}$ [where L = 4-(dimethylamino)pyridine (**1**), pyridine (**2**), 3-cyanopyridine (**3**), or 4-cyanopyridine (**4**), and pz = pyrazine],[2−6] Figure 1. These complexes display rich mixed-valence behavior that is "tunable" via changes in the ancillary pyridyl ligands L, including large comproportionation constants evident by cyclic voltammetry and relatively high-energy near-infrared/visible electronic absorption bands that have been assigned as "intervalence" absorption bands.

The unique spectral feature of these complexes is the partial coalescence of cluster-bound carbonyl infrared (IR) bands, where the degree of coalescence is correlated with the strength of electronic communication as quantified in other measurements. The fact that the carbonyl IR bands are not completely coalesced allows $\mathbf{1}^-$−$\mathbf{4}^-$ to be classified as localized complexes on the vibrational time scale. The shape of the partially coalesced bands has been used to determine thermal intramolecular electron-transfer rates of $10^{11}-10^{12}$ s^{-1}. The quantitative experimental determination of such fast, thermal, and zero-driving-force electron-transfer rates is unprecented save in these complexes. The observation of electron transfer on the time scale for dynamic infrared band coalescence in $\mathbf{1}^-$−$\mathbf{4}^-$ has facilitated

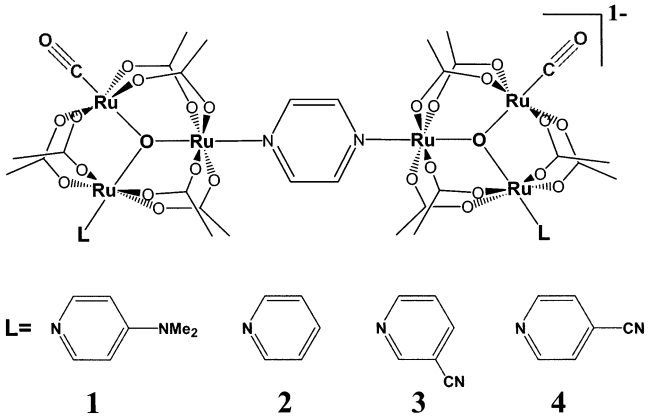

Figure 1. Pyrazine-bridged dimers of trinuclear ruthenium clusters. The singly reduced states are mixed-valence charge-transfer complexes.

investigation of other aspects of mixed-valence behavior in the near-delocalized, low thermal barrier limit: the strong dependence of ET rates on fast dipolar solvent relaxation has been documented,[4] and the utility of IR-active symmetric bridge vibrations for assignment of localization or delocalization has been questioned.[5]

Mixed-valency, even in the near-delocalized limit, is typically discussed in terms of the semiclassical Hush adaptation of the Marcus theory of ET.[7] The celebrated and much-discussed Creutz−Taube ion,[8] $[(NH_3)_5Ru(\mu\text{-pz})Ru(NH_3)_5]^{5+}$, is an example of a mixed-valence system that appears to exceed the bounds of explanation by Marcus−Hush theory and is generally agreed to be delocalized.[9] An important advance in the understanding of the Creutz−Taube ion was the application of a three-state, vibronic model for its electronic structure and the subsequent verification of experimental predictions of this model in resonance Raman spectroscopy.[10,11] A recent study of

* Corresponding author. E-mail: ckubiak@ucsd.edu.

10.1021/jp035643q CCC: $25.00
Published on Web 10/15/2003

asymmetrically substituted mixed-valence clusters of the same type as $\mathbf{1}^{-}-\mathbf{4}^{-}$ is presented in terms of Marcus−Hush theory but calls into question the applicability of the theory to near-delocalized (but clearly still partially localized) complexes of this type.[12] It is shown here that the three-state vibronic model is directly applicable in $\mathbf{1}^{-}-\mathbf{4}^{-}$ and should be considered as a more realistic model than the semiclassical, two-state Marcus−Hush theory or even two-state vibronic models for bridged, near-delocalized mixed-valence complexes.

1.2. Vibronic Coupling Models Applied to Mixed-Valence Complexes. Since the synthesis of the Creutz−Taube ion,[8] and with many literature reports of mixed-valence complexes displaying intervalence-transfer (IT) electronic absorption bands, vibronic models that include molecular normal coordinates assumed to be important for electron transfer have been used to rationalize the nature of these IT bands and the electronic structure of mixed-valence complexes.

The first, two-site vibronic model[13] for ET in mixed-valence complexes, proposed by Piepho, Krausz, and Schatz and subsequently referred to as the PKS model, incorporated a small-polaron coupling of one vibration on each of two sites to model self-exchange electron transfer. The only vibrations considered were the fully symmetric breathing modes of each charge center. Linear combinations of these single-site modes give the intramolecular electron-transfer coordinate (the antisymmetric combination mode), *q*, and the symmetric combination mode, *Q*. This model was extended to include multiple single-site modes[14,15] and solvent effects,[16] and its consequences were explored in terms of predicted line shapes of IT bands and postulated "tunneling" far-infrared absorptions,[17] which subsequently were shown not to exist in the Creutz−Taube ion.[18] The similarities of this model to linear-response theory as applied to small-polaron coupling cases have been noted,[19] and it was claimed[20] that this model successfully accounts for vibronic enhancement of symmetric TCNQ normal modes in organic linear-chain conductors,[21−26] which were typically analyzed using adapted linear-response theory.

The main shortcoming of the PKS model as applied to mixed-valence complexes (rather than nonbridged dimeric ions such as $TCNQ_2^{-}$), as pointed out originally by Hush,[27] is that it neglects the central importance of the bridging ligand in mediating the electronic communication between charge centers in the limit that there is no direct orbital overlap between them. A time-dependent, two-state model similar to PKS theory but incorporating metal-bridge vibrations rather than symmetric charge site breathing modes has been proposed by Zink et al. to simulate IT band shapes and resonance Raman intensities of coupled metal-bridge vibrations.[28−30] However, it is a three-state vibronic coupling model that explicitly includes an electronic state localized on the bridging ligand that is needed to explain the IT band shape and resonance Raman profile[10,11,31,32] of the Creutz−Taube ion. The work of Ondrechen and others[31−45] has expanded this model, which began as a simple three-site propagator model, to include not only the two fully symmetric charge-site modes mentioned above but also symmetric bridge vibrations and potentially dynamic solvent effects.

2. Application of the Three-State Model to Hexaruthenium Mixed-Valence Complexes

The Ondrechen three-state model, with vibronic coupling of bridge vibrations to the "IT" band, has been recently proposed as an explanation for the IR activity of symmetric pyrazine bands in $\mathbf{1}^{-}-\mathbf{4}^{-}$.[5] The proposed model is also consistent with the observed resonant enhancement of the same bands in resonance Raman spectroscopy with excitation in the IT bands of these complexes.[6] In this section, a full consideration of the electronic structure and molecular orbitals in the trinuclear ruthenium clusters of interest, aided by molecular orbital and normal mode calculations, shows the specific applicability of the three-state model to $\mathbf{1}^{-}-\mathbf{4}^{-}$. A careful consideration of the important molecular orbitals on both the trinuclear clusters and their ligands helps to elucidate both the orbital basis for electronic delocalization and the nature of the resultant, delocalized electronic states of both "monomeric" trinuclear clusters and $\mathbf{1}^{-}-\mathbf{4}^{-}$. These "ET basis state" molecular orbitals and the transformed, delocalized electronic linear combination states, combined with an analysis of the molecular vibrations important to electron transfer and mediation of electronic delocalization through the pyrazine bridge, lead to specific experimental predictions for $\mathbf{1}^{-}-\mathbf{4}^{-}$.

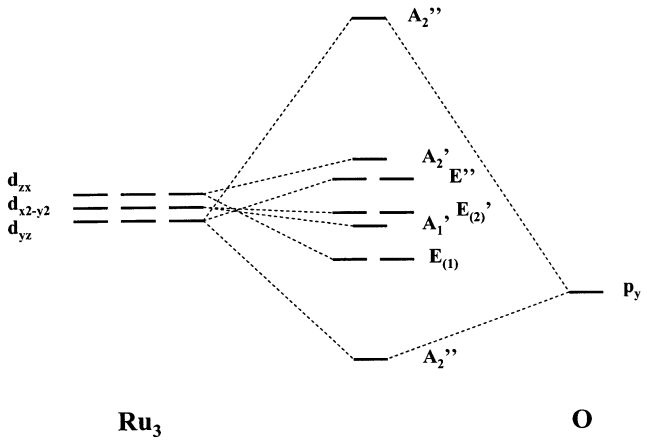

Figure 2. Qualitative π molecular orbital scheme for a trinuclear ruthenium cluster with three identical ancillary ligands L, $Ru_3(\mu_3\text{-}O)(OAc)_6L_3$ (D_{3h} symmetry). The local *z* axis of each pseudo-octahedral Ru center lies along its Ru−(μ_3−O) bond, and the *y* axes lie perpendicular to the Ru_3O plane. For a cationic cluster ($Ru_3^{III,III,III}$) with 15 metal d electrons and two from O, all levels except the highest A_2' orbital (single electron occupation) and the antibonding A_2'' orbital (empty) would be occupied.

2.1. Electronic Structure of Trinuclear Ruthenium Clusters. The molecular orbitals of trinuclear, carboxylate-bridged ruthenium clusters have typically been taken to follow a scheme[46−48] that incorporates specific d orbitals on each Ru atom and what is chosen as the p_y orbital of the μ_3-bridging O atom to form an extended dπ system.

Figure 2 shows the anticipated orbital symmetries and qualitative relative energies for a trinuclear cluster with three identical ancillary (axial) ligands (D_{3h} symmetry). Figure 3 compares the related orbital scheme for a lowered-symmetry (C_{2v}) case when one of these ligands is unique, as in the case of a monocarbonylated cluster with two pyridine ligands. In both cases, the highest energy cluster molecular orbital in this scheme is the antisymmetric linear combination of three ruthenium dπ orbitals and the p_y oxygen orbital. This delocalized, cluster antibonding orbital is expected to be of the right symmetry, energy and spatial orientation to overlap well with the π* orbitals of π-acid ligands (like CO and isocyanides) and conjugated N-heterocycle ligands (like pyridine and pyrazine).

Further lowering of symmetry (to C_s in the case of three different cluster ligands such as L_1 = CO, L_2 = pyridine and L_3 = pyrazine) leaves the same dπ* orbital biased toward greater occupation on the Ru atom coordinated to one pyridyl ligand or the other but unchanged in its delocalized character. Explicit

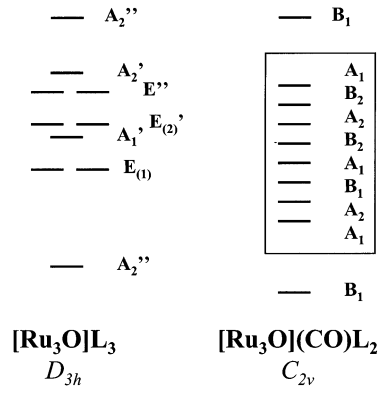

Figure 3. Comparison of π molecular orbital schemes for trinuclear ruthenium clusters in (D_{3h} symmetry, from Figure 2), and with one carbonyl ligand (C_{2v} symmetry), i.e., $Ru_3O(OAc)_6(CO)(pyridine)_2$. In the lower symmetry case, relative energies of intermediate cluster orbitals are more difficult to specify so these states are grouped into a "band" structure for graphical purposes. In a neutral C_{2v} cluster (formally $Ru_3^{III,III,II}$), all orbitals would be occupied except the antibonding B_1 orbital.

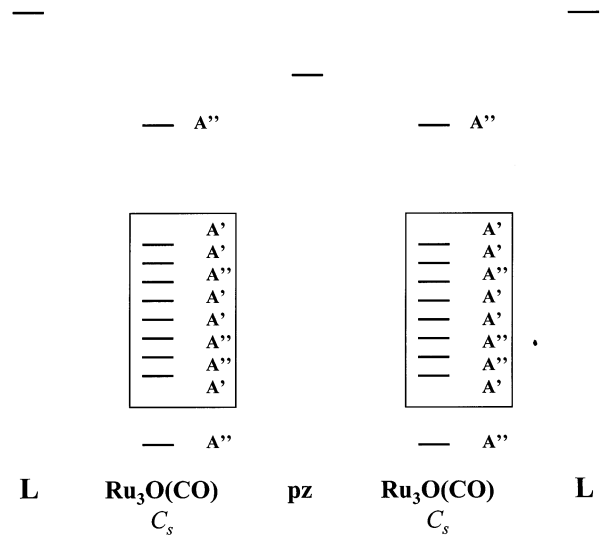

Figure 4. π molecular orbital scheme for two trinuclear ruthenium clusters bridged by pyrazine, i.e., **1**−**4** (with C_s local symmetry at clusters and C_{2h} overall molecular symmetry in the absence of any charge localization effects). Only the pyridine (py) and pyrazine (pz) π^* orbitals important to interaction with the highest lying cluster antibonding state are shown. A mixed-valence (−1) state would have full electronic occupation of the cluster "bands" and one additional electron in an occupational exchange between the cluster antibonding orbitals and the pyrazine π^* orbital.

inclusion of the empty CO π^* orbital into this delocalized cluster orbital and momentary neglect of interactions with N-heterocycle ligands gives the orbital picture shown in Figure 4 for a "dimer of trimers" bridged by pyrazine with identical ancillary pyridyl ligands.

2.2. Molecular Orbitals on Clusters and Pyrazine: Three Electronic Basis States. The three-state model assumes three electronic basis states with parametrized interactions between them. When the model is applied to $\mathbf{1}^-$−$\mathbf{4}^-$, these three states should include two cluster-based states and one bridge-based electronic state. The two cluster states are assumed only to interact with each other through the bridge-based state. In a symmetric mixed-valence system, the important electronic parameters are *J*, the exchange coupling between each of the charge center states and the bridge state, and α, the energy gap between the charge center states and the bridge state (Figure

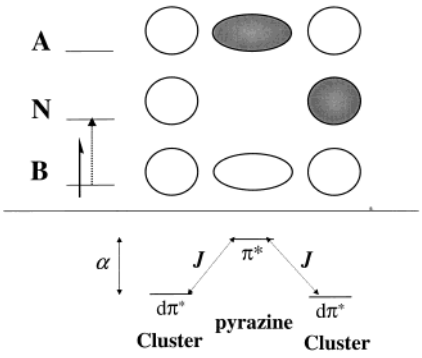

Figure 5. Schematic of electronic basis states of the three-state model with independent parameters *J* (exchange coupling between cluster and bridge) and α (energy difference between cluster-based and bridge-based states), with the three resultant molecular orbitals. The symmetric combination level is "B" or bonding, the antisymmetric combination "A" or antibonding, and the intermediate energy level with a node on the bridging ligand is "N" or nonbonding. Electronic occupation for a (−1) mixed valence state of **1**−**4** is shown. The symmetry-allowed electronic transition, B → N, is shown with a dotted arrow. These "molecular orbitals" are analogous to the π orbitals of the allyl radical (but the electronic occupation is different).

5). From the three electronic basis states and assuming significant exchange coupling between them, a three-state delocalized π system can be constructed as shown in Figure 5, for which the lowest energy "molecular orbital" is the symmetric combination of the three electronic basis states.

The relative simplicity of this three-state Hückel-type model has been criticized[32] in the case of the Creutz−Taube ion, partially due to anticipated problems with near-degenerate Ru d orbitals on each Ru and the possibility of spin−orbit coupling interactions. However, density functional calculations for a "monomeric" trinuclear cluster suggest that a model invoking only three electronic states (electronic occupation in a single molecular orbital on each cluster and in a single orbital on the bridging pyrazine ligand) should be reasonably valid in the case of $\mathbf{1}^-$−$\mathbf{4}^-$. According to the qualitative molecular orbital scheme presented above for these trinuclear clusters, only one cluster orbital (the delocalized cluster antibonding orbital) should have a significant exchange coupling interaction with the bridging ligand π^* level, due to the small energy gap and good spatial overlap between this cluster orbital and the π^* orbital of pyrazine.

Molecular orbital calculations (see section 7.1) on a single trinuclear cluster with two pyridine ligands, $Ru_3O(OAc)_6(CO)(pyridine)_2$, show that the LUMO in a $Ru_3^{III,III,II}$, neutrally charged cluster and the HOMO in a $Ru_3^{III,II,II}$, (−1)-charged cluster is indeed a delocalized, dπ^*-type orbital that is delocalized over the entire cluster (all three ruthenium atoms and the μ_3-O atom) and parallel to the plane of the ruthenium and μ_3-O atoms (Figure 6).

This is the antisymmetric combination of the ruthenium d_{yz} and oxygen p_y orbitals postulated in qualitative schemes discussed earlier (Figures 2 and 3) to be the (0) LUMO. It is important in Figure 6 to note the overlap of this delocalized cluster orbital with both the cluster carbonyl π^* orbital and the largely N-based π^* orbitals of pyridine or pyrazine ligands. The cluster carbonyl ligand C−O stretching frequency is extremely sensitive to the charge of the cluster, and this orbital picture provides the expected basis for such sensitivity via π-backbonding to the CO ligands. Electronic occupation in this cluster orbital is also expected to easily flow into the π^* orbital of a bound pyrazine ligand and lead to a large exchange coupling

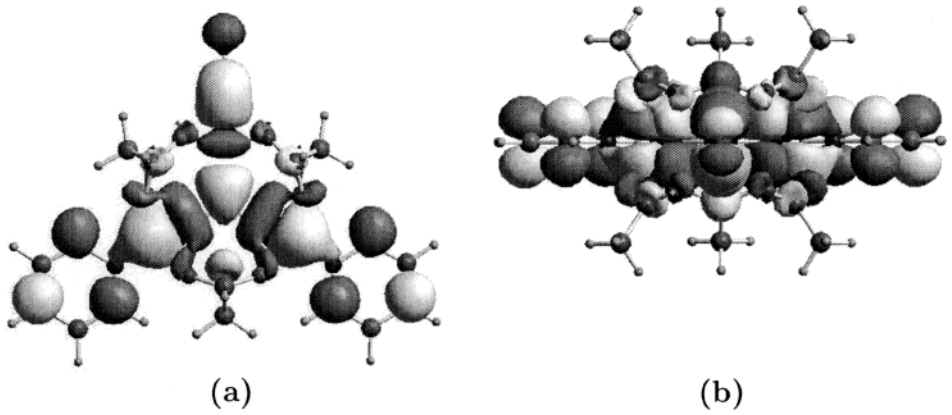

Figure 6. Calculated LUMO of $Ru_3O(OAc)_6(CO)(pyridine)_2$. (a) "Top" view: cluster-bound carbonyl ligand is top center. (b) "Side" view, looking down the O−C−Ru bond of the cluster-bound carbonyl ligand.

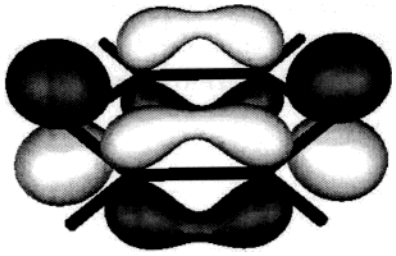

Figure 7. π^* orbital and LUMO of pyrazine. N atoms are at the left and right of the stick structure.

between a bridge-based radical electronic state and cluster states with single electronic occupation in the dπ^*-cluster orbitals.

According to the DFT calculations (and the cited qualitative MO schemes), no other cluster orbitals are close enough in energy nor spatially overlapping enough with the N-based pyrazine π^* orbital (the pyrazine LUMO) to significantly influence its electronic occupation. The π^* orbital of pyrazine is well-known, and it is best represented as what is mainly a symmetric combination of the N-based p orbitals involved in the pyrazine π system (see Figure 7).

In a simple picture and for the purposes of the three-state model, the (−1) state of **1**−**4** can be viewed in terms of a single electron exchanging between three states: two with the electron in cluster-based dπ^* orbitals, and one with the electron in the higher energy π^* orbital of the bridging pyrazine ligand. Thus, a single-electron Hückel Hamiltonian is expected to accurately reflect the electronic properties of this particular three-site system without the need for augmentation to higher levels of theory. It is of interest to note that this single-electron occupation differs from the electronic occupation in the three-state model applied to the Creutz−Taube ion, which has a total of three electrons in the three molecular orbitals of interest and thus for best accuracy must be treated using a more sophisticated Hubbard Hamiltonian that takes the energetic effects of electron exchange and correlation in the transformed molecular electronic states into account.[32,42,44]

2.3. "Intervalence" Bands and the Role of the Pyridyl Ancillary Ligands. The "intervalence" band anticipated for $\mathbf{1}^-$−$\mathbf{4}^-$ on the basis of the arguments presented thus far is expected to be more like an electronic transition between the "B" and "N" levels of the three-state model (Figure 5), and in this facet of their spectroscopy, $\mathbf{1}^-$−$\mathbf{4}^-$ should be similar to the Creutz−Taube ion. At this point, however, it is important to note that although the favorable overlap between the important cluster antibonding dπ^* orbital and the π^* LUMO of pyrazine has been considered, the less energetically favorable but equally

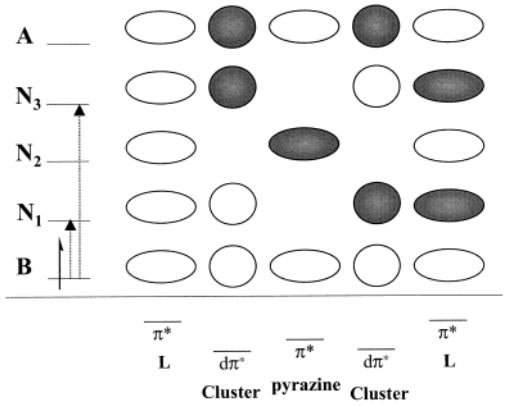

Figure 8. Qualitative molecular orbitals of a five-state model for electronic delocalization in $\mathbf{1}^-$−$\mathbf{4}^-$, with electronic occupation expected for the (−1) mixed-valence species. Energy gaps between states and relative energies of states are not necessarily accurate due to possible energy gap effects. Two symmetry-allowed electronic transitions for the single electron are expected: B → N_1 and B → N_3. Relative energies are not necessarily to scale.

spatially favorable overlap between the pyridine π^* orbitals and the dπ^* orbitals of the clusters to which they are bound has not been included. If an exchange coupling interaction of the same order of magnitude as the [dπ^*(cluster) ↔ π^*(pyrazine)] interaction is assumed, then the delocalization of the single electron in the three-state model of Figure 5 should be better described by a single-electron, *five*-state electronic model that also includes basis states with the electron in the π^* orbital of each ancillary pyridyl ligand. The molecular orbitals predicted by a five-state scheme are shown in Figure 8. The Hückel-type linear combination orbitals of the five-state model are reminiscent of the molecular orbitals of the pentadienyl radical in the same way that the molecular orbitals of the three-state model resemble those of the allyl radical.

The orbitals and electronic behavior predicted in the five-state model are not a large departure from the three-state model. Single-electron occupation still describes the system, and the ground electronic state has the electron in a fully symmetric linear combination, "B" or bonding state. Now two electronic transitions are allowed by symmetry, the B → N_1 and B → N_3 transitions, both of which have the same basic properties as the B → N transition in the three-state model: the electronic excited states each have a node on the bridging ligand and the transitions are expected to be partially ligand-to-metal charge transfer in character (again rather than "intervalence" or metal-to-metal charge-transfer character). In a sense, the two allowed transitions in the five-state model are like the single B → N transition in

the three-state model but "split" in energy by electron exchange interactions with the ancillary pyridine ligands' π^* levels. The "N_1" and "N_3" molecular orbitals of the five-state model are like "symmetric" and "antisymmetric" combinations of the original "N" orbital in the three-state model with the two pyridine π^* orbitals.

The prediction of the five-state electronic model of two "intervalence" or B → N transitions actually matches the electronic spectra of $\mathbf{1}^{-}-\mathbf{4}^{-}$ well, because two near-infrared bands are observed for each of these mixed-valence clusters (one centered at approximately 6000 cm^{-1} and one at approximately 11 000 cm^{-1}), both with similar spectral bandwidths.[3] The previous assignment of the higher energy of the two bands as the "IT" band is tentatively called into question, as the qualitative five-state model presented here appears to predict that *both* bands should be, in a sense, parts of the "IT" band or three-state B → N transition that is typically observed in near-delocalized mixed-valence complexes. Although the resonance Raman investigation reviewed in section 4.1 is centered on the higher energy near-IR band, it is suggested here that the vibronic signatures of either of the near-IR transitions should be qualitatively identical. Further investigation of the lower energy band is clearly in order, but for the purposes of this paper the higher energy band (which the five-state model would say is the B → N transition) will be considered to be the "IT" band or B → N transition in the three-state model and the participation of the pyridine π^* orbitals will be formally neglected.

The intent here is to highlight the importance of a *vibronic* model for $\mathbf{1}^{-}-\mathbf{4}^{-}$ that explicitly includes the bridging ligand, and the electronic participation of other ligands is of secondary concern to this argument (although it is potentially very important in a complete description of the electronic spectroscopy of these complexes). The three-state model (rather than the full five-state treatment) will be discussed exclusively in the following sections. As mentioned in section 5, the important role in terms of electron-transfer activity of varying the ancillary ligands L is to adjust the energy gap α between cluster- and bridge-based electronic states. This modulation of the energy gap in the three-state model provides synthetic control of the thermal intercluster ET rate.

2.4. Important Molecular Vibrations. The vibrations included in the three-state vibronic model can in principle include any of the normal modes of a mixed-valence complex. In the case of the Creutz−Taube ion, which is generally accepted to be delocalized, or Robin−Day[49] class III, the most important modes for calculation of the B → N (or IT) electronic absorption profile have been taken to be of five types, shown schematically in Figure 9. The importance of *symmetric* modes in mediating communication between charge sites is a significant realization of vibronic models for site-to-site ET. All molecular vibrations enter the three-state model parametrically through vibronic coupling constants, A_i, for each *i*th vibration.

2.4.1. Cluster Breathing Modes and Cluster−Ligand Stretching Modes. There has been some discussion[10,11,14,27,50] of the relative importance in vibronic ET models of localized charge site breathing modes versus charge site-bridging ligand stretching modes. In the PKS formulation applied to the Creutz−Taube ion,[13] the important modes were assumed to be the symmetric Ru−ammine stretching modes, because there is a significant change in all Ru−N bond distances upon electron transfer and a change in oxidation state from Ru^{II} to Ru^{III}. Symmetric, *Q*, and antisymmetric, *q*, linear combinations of these modes were considered. In a bridged system, the charge-site-bridging ligand

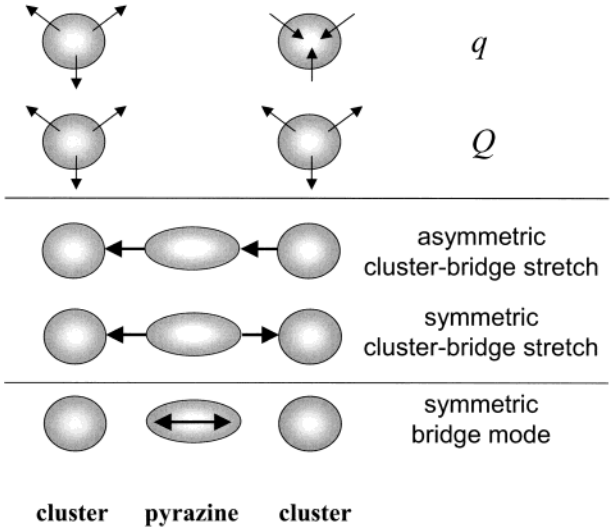

Figure 9. Important molecular vibrations in the three-state model for electron transfer and delocalization.

TABLE 1: Selected Calculated Frequencies (B3LYP/LANL2DZ) of $Ru_3O(OAc)_6(CO)(pyridine)_2$, C_{2v} Symmetry[a]

frequency (cm^{-1})	symmetry	assignment
154 (156)	A_1	symmetric cluster breathing
208 (207)	B_1	asymmetric cluster−pyridine stretch
203 (210)	A_1	symmetric cluster−pyridine stretch
1954 (1956)	A_1	C−O stretch

[a] Numbers in parentheses are for an alternate structure with the pyridine rings rotated 90° out of the Ru_3O plane.

bond length is also expected to change with the charge site oxidation state due to electron transfer; because the bridging ligand mediates the electronic interaction between charge sites, it has been argued that the most important normal modes to consider should be the two charge-site-bridging ligand stretching modes, also in symmetric and antisymmetric linear combinations.

The electron-transfer coordinate is expected to be defined along antisymmetric combination modes of the two types discussed above. Because we are not currently able to report detailed low-frequency IR or Raman spectra due to existing experimental limitations (see section 7), the relative importance of cluster−bridging ligand stretching modes and symmetric cluster breathing modes cannot be discussed meaningfully at this time. However, frequency calculations on model trinuclear complexes do help to elucidate the frequencies of the normal modes that should be important in the three-state vibronic model for $\mathbf{1}^{-}-\mathbf{4}^{-}$.

Frequency calculations (Table 1) on the "monomeric" ruthenium cluster complex with two pyridine ligands (described in section 2.2) find two cluster−pyridine stretching modes. The small difference in frequency between them highlights the lack of vibrational coupling between the cluster−ligand stretching motions of two ligands coordinated to the same cluster. On the basis of these calculated frequencies, it can be assumed that with N-heterocyclic pyridine-type ligands such as pyridine and pyrazine, the cluster−ligand stretching frequencies for these clusters are close to 200 cm^{-1}. These frequencies are lower than but similar to metal−pyrazine stretching frequencies for the Creutz−Taube ion,[51] and they are also notably close to *kT* at solution−sample experimental temperatures.

The fully symmetric cluster breathing mode for the "monomeric" complex is calculated as 154 cm^{-1};[52] this frequency is less than one-third of the ∼500 cm^{-1} symmetric Ru−ammine

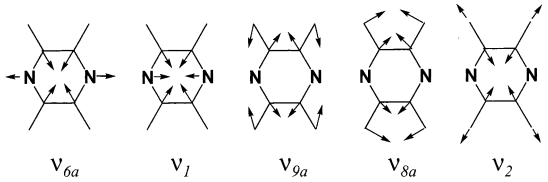

Figure 10. Fully symmetric normal modes of pyrazine in order of increasing frequency.

breathing mode frequency for the Creutz−Taube ion,[51] and also low enough in energy that significant thermal population of its first vibrational excited state would be expected at liquid-phase temperatures. These calculated "monomer" frequencies suggest that compared to mixed-valence complexes with mononuclear charge sites such as the Creutz−Taube ion, the potential surface for intercluster ET in $\mathbf{1}^-$−$\mathbf{4}^-$ (which is expected to proceed along a combination of antisymmetric cluster−bridging ligand and cluster breathing modes, because both types of adjustments should occur upon electron transfer) is much "softer" with greater possibility for thermal population of excited vibrational states in vibrations important to the electron-transfer process. The symmetric linear combination vibrations are expected to act as low-frequency mediators of site-to-site electronic interactions. Most specifically, the symmetric combination of cluster−ligand stretching modes is expected to directly mediate exchange coupling between the bridging ligand and both clusters, and thus it should also mediate electronic communication between clusters. As electron transfer between clusters becomes less important and electronic delocalization becomes a dominant factor (the Robin-Day Class II/III or localized-to-delocalized transition), the symmetric cluster−bridge stretching mode is expected to become vibronically dominant and the antisymmetric modes should lose importance in the overall electronic behavior of a mixed-valence cluster like $\mathbf{1}^-$−$\mathbf{4}^-$.

2.4.2. Symmetric Bridging Ligand Modes. In a model that explicitly includes an ET basis state localized on the bridging ligand, symmetric bridging ligand normal modes should be of great importance in mediating both the "basis" site-to-site ET process and the "transformed" delocalized electronic structure. Qualitatively, symmetric bridging ligand modes are expected to have the same effect as the symmetric cluster−bridging ligand stretching mode in mediating electronic communication between clusters through the bridging ligand. In this way, they should be vibronically linked to electronic processes involving cluster−bridge and cluster−cluster interactions.[53]

Pyrazine (D_{2h} symmetry) has five fully symmetric (A_g) normal modes (Figure 10).[54,55] In the context of pyrazine-bridged mixed-valence complexes, the lowest frequency symmetric mode (ν_{6a}) has been assumed to be the most important in mediating the electronic interaction between clusters.[31] The ν_{8a} mode has been the subject of discussion as a possible probe of dynamic charge localization.[1] The highest frequency symmetric C−H stretching mode (ν_2) does not significantly alter the N−N distance in pyrazine and is likely of minor importance in mediating the electronic interaction between coordinated clusters through the π^* orbital. Spectroscopic observations detailed below show that the modes ν_1, ν_{9a}, and ν_{8a} are all vibronic participants in electronic delocalization in the ruthenium "dimers of trimers" vis-a-vis the three-state model.[56]

3. Vibronic Coupling and Predictions of the Three-State Model

The B → N electronic transition in the three-state model replaces what is conventionally thought of as the intervalence absorption band in strongly interacting mixed-valence complexes. In the widely used two-state, semiclassical Marcus−Hush formalism,[7] the energy of the IT absorption band is taken to be λ, the reorganization energy for electron transfer from the first site to the second at the nuclear coordinates corresponding to the electron's localization at the first site. In the three-state model, the energy of this transition is[41]

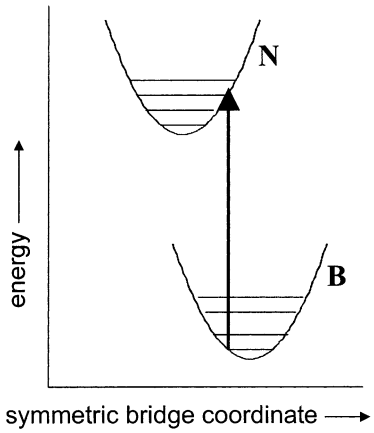

Figure 11. Vibronic coupling of a symmetric bridge vibration to the B → N electronic transition. Because the transition involves partial electron transfer from the bridging ligand clusters, there is a significant shift along the symmetric coordinate between the minima for the ground (B) and excited (N) electronic states.

$$E_{B\rightarrow N} = -\frac{1}{2}(\alpha - \sqrt{\alpha^2 8J^2}) \qquad (1)$$

and is thus expected to reflect mainly the exchange coupling, J, in the limit of large exchange coupling and a relatively small energy difference α between cluster and bridge basis states. This key difference between the two-state semiclassical formalism and the vibronic model presented here in the description of the "intervalence" band qualitatively explains how a near-delocalized mixed-valence system with very low reorganization energy for electron transfer can still exhibit a high-energy (near-IR or visible) "IT" band.

If the three-state Hückel molecular orbital system shown in Figure 5 is occupied by a single electron, the only allowed electronic transition is the B → N transition. Because the N electronic state has a node on the bridging ligand, this electronic transition has the character of a pyrazine-to-two clusters charge-transfer transition, or ligand-to-metal charge transfer (LMCT). This transition is expected to involve a significant nuclear adjustment along symmetric pyrazine normal coordinates due to the *strengthening* of the pyrazine bonds associated with depletion of electron density in the pyrazine π^* orbital, and thus symmetric pyrazine modes (as well as the symmetric cluster−pyrazine combination mode) should be vibronically coupled to the B → N transition. This is schematically illustrated in Figure 11.

Because the "B" state involves partial electronic occupation in the π^* orbital of pyrazine, a simple prediction of the model applied to $\mathbf{1}$−$\mathbf{4}$ is that symmetric pyrazine modes in the (−1) mixed-valence species should exhibit lower frequencies than in the (0) isovalent states, which have no electronic occupation in pyrazine antibonding orbitals. This frequency shift upon reduction was clearly observed in Raman results.[6] With regard to symmetric modes of the bridging ligand, the vibronic coupling to the B → N transition should have specific experimental consequences. The most obvious is that resonance Raman experiments with excitation in the B → N transition are expected

to show significant resonant enhancement of symmetric bridge modes. A wave packet placed on the excited state (N) surface at the coordinates of the minimum of the ground state (B) surface is expected to evolve significantly along symmetric bridging ligand normal coordinates toward the displaced energy minimum of the N surface. Observation of this predicted resonant enhancement of symmetric bridging ligand modes was documented in both the Creutz−Taube ion[10,11] and more recently in $\mathbf{1}^-$, $\mathbf{2}^-$, and $\mathbf{4}^-$ (see section 4.1).[6]

A more subtle effect of the mixing of vibrational and electronic transitions through vibronic coupling in the three-state model is the possibility of dipole activity in formally dipole-forbidden vibrational transitions. Due to vibronic coupling to the B → N transition and to vibronic mixing of states in the three-state model, the coupled normal modes (including symmetric bridging ligand modes) acquire "pieces" of the electronic excited state in their vibrational wave functions. From the point of view of one symmetric bridge mode, what is nominally the $|\nu = 0\rangle \rightarrow |\nu = 1\rangle$ transition becomes no longer just a simple vibrational transition due to vibronic mixing of the $|B, \nu = 0\rangle$ and $|B, \nu = 1\rangle$ wave functions with excited-state wave functions such as $|N, \nu = 0\rangle$, $|N, \nu = 1\rangle$, $|N, \nu = 2\rangle$, etc. The result of this mixing is that the nominally $|B, \nu = 0\rangle \rightarrow |B, \nu = 1\rangle$ vibrational transition can acquire dipole activity from the electronic transition to which it is coupled. This argument was alluded to by Zhang et al.[41] and suggests that the observation of formally forbidden bridging ligand modes in IR spectra is a marker of vibronic coupling and three-state interaction in mixed-valence complexes such as the Creutz−Taube ion and $\mathbf{1}^-$−$\mathbf{4}^-$, rather than simply a probe of localization or delocalization in the Robin−Day class II/class III sense.[1,49]

4. Spectroscopic Validation of the Three-State Model: Vibronic Activity of Bridging Ligand Modes

4.1. Resonance Raman Enhancement of Symmetric Pyrazine Modes. Using an excitation wavelength of 752 nm, which is post-resonant with the near-IR/visible electronic band assigned as the "IT" band for $\mathbf{1}^-$, $\mathbf{2}^-$, and $\mathbf{4}^-$, resonant enhancement of three symmetric pyrazine modes (ν_1, ν_{9a}, and ν_{8a}) was recently demonstrated.[6] This observation confirms the most obvious prediction for the vibronic activity of symmetric bridging ligand modes. The most enhanced of the three modes mentioned appears to be ν_{8a}. The ν_{6a} mode is overlapped by a solvent peak at approximately 700 cm^{-1} and will require investigation in a different solvent to clarify its relative enhancement.

Besides the resonant enhancement of the symmetric pyrazine modes in the (−1) mixed-valence states, the frequency shifts between the (0) and (−1) states in the symmetric pyrazine modes are significant. Each pyrazine mode also exhibits a markedly lower frequency in the reduced state due to partial electronic occupation of the pyrazine π^* orbital in the "B" electronic state, as predicted by the model in section 3.

4.2. Infrared Activity of Symmetric Pyrazine Modes. The observation of a strong peak corresponding to the ν_{8a} symmetric mode of pyrazine in the (−1) mixed-valence state of $\mathbf{1}$−$\mathbf{4}$ was recently reported.[5] This mode was assigned by substituting pyrazine-d_4 for pyrazine-h_4 and documenting the characteristic frequency shift.[54,55] Further inspection of the (−1) IR spectrum outside the C−O stretching region reveals similar (but much weaker) IR activity in the ν_1 and ν_{9a} modes, but these peaks are somewhat difficult to distinguish from electrolyte and solvent subtraction artifacts and would not be identifiable without isotopic substitution (of pyrazine-d_4) and a previous knowledge of their exact frequencies in the (−1) species from Raman experiments. The clearest IR probe of the behavior of the symmetric pyrazine vibrations is the ν_{8a} band, although this behavior appears to be qualitatively similar in all three of the pyrazine symmetric modes observed in the infrared spectra of these complexes.

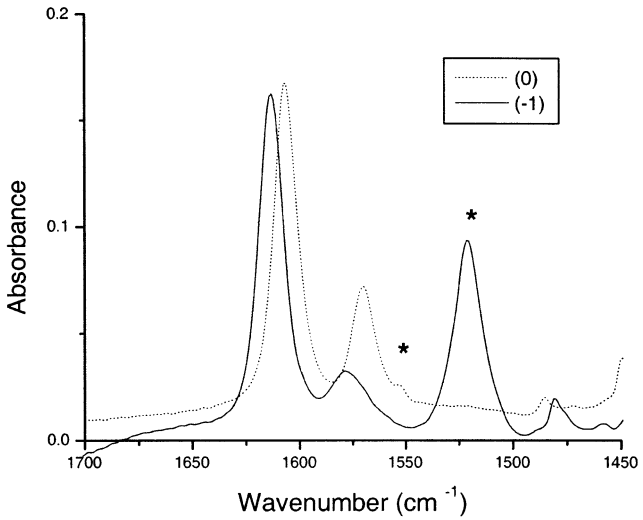

Figure 12. Infrared spectra of $\{Ru_3O(OAc)_6(L)(CO)\}$pyrazine-d_4, **5**, where L = pyridine. Dotted line: (0) state. Solid line: (−1) state. Peaks assigned to ν_{8a} of pyrazine are marked with an asterisk.

Infrared activity in the ν_{8a} mode in pyrazine-bridged Ru and Os mixed-valence complexes has been interpreted as a marker for localization of charge on a time scale longer than one period of the mode, ca. 20 fs.[1] Very little difference in extinction coefficient for the ν_{8a} absorption band is observed in the series $\mathbf{1}^-$−$\mathbf{4}^-$, suggesting that (1) the origin of IR activity in each of the mixed-valence complexes is qualitatively the same, and (2) if the origin of the infrared intensity is vibronic coupling, then there is very little difference between the vibronic coupling constants for complexes with different strengths of electronic communication. More telling is a comparison to nonmixed-valence complexes with intentionally asymmetric coordination environments for pyrazine. In the complexes $\{Ru_3O(OAc)_6(L_1)(CO)\}(\mu\text{-pz})\{Ru_3O(OAc)_6(L_2)(CO)\}$, where $L_1 \neq L_2$,[12] a pattern identical to that seen in $\mathbf{1}$−$\mathbf{4}$ is observed: the ν_{8a} pyrazine vibration is apparently only IR-active in the (−1) states. Isotopic subsitution of the bridging pyrazine ligand was not carried out for these complexes, so the ν_{8a} band could be weakly active in the isovalent (0) and (−2) species but obscured by overlapping bands from acetate and pyridyl ligand modes. Regardless of any obscured weak bands, the lack of obvious ν_{8a} activity in the isovalent (0) and (−2) species in the asymmetric dimers shows that simple coordination asymmetry at pyrazine does *not* lead to strong IR activity in the symmetric ν_{8a} band of pyrazine in ruthenium "dimers of trimers" like $\mathbf{1}^-$−$\mathbf{4}^-$.

Spectroelectrochemical investigation of a "monomeric" trinuclear complex with one isotopically substituted pyrazine ligand, $\{Ru_3O(OAc)_6(L)(CO)\}$pyrazine-d_4, **5**, where in this specific case L = pyridine, exhibits curious behavior in the region of the ν_{8a} absorption band for pyrazine-d_4 (Figure 12). In this complex, pyrazine has an extremely asymmetric coordination environment: coordinated at one nitrogen atom and not coordinated at the other. In the (0) state of this complex, there may be evidence of very weak IR activity in the ν_{8a} mode of pyrazine in a shoulder at 1554 cm^{-1}. However, in the (−1) state, the mode is *strongly* active and shifted to much lower frequency (1521 cm^{-1}). Even in such a specifically asymmetric coordination environment, IR activity in the ν_{8a} mode of pyrazine appears to be influenced mainly by vibronic factors.

In the (−1) state of **5**, the (−1) electron presumably resides in the dπ* delocalized cluster orbital described in section 2.2. An electron in this cluster molecular orbital is expected to experience significant stabilization (exchange coupling) through orbital overlap with the unoccupied π* orbital of pyrazine, and this large overlap and sharing of the (−1) charge is evident in the negative frequency shift of the ν_{8a} pyrazine band between the (0) and (−1) states of **5**. Vibronic activity in this exchange coupling, between specific cluster and pyrazine orbitals and in the presence of a single electron occupying electronic states that are mixed linear combinations of these orbitals, appears to be the main source of infrared activity in the ν_{8a} mode of pyrazine. Strong infrared activity in otherwise weak or symmetry-forbidden normal modes appears to be one of the vibronic consequences of this significant mixing of adjacent pyrazine- and cluster-based electronic states.[57] The possibility that dipole activity could be acquired by symmetric pyrazine modes in the more symmetrically coordinated "dimer" mixed-valence species $\mathbf{1}^{-}-\mathbf{4}^{-}$ seems more likely in light of this example, and the pyrazine-bound "monomer" IR results for **5** clearly rule out asymmetry at pyrazine as a major source of IR activity of these modes in $\mathbf{1}^{-}-\mathbf{4}^{-}$.

The "monomeric" cluster pyrazine complex **5** shows that symmetric pyrazine modes can acquire IR activity due to vibronic coupling and the presence of a large exchange coupling in which one electron is shared between specific molecular orbitals (the dπ* cluster orbital and the π* orbital of pyrazine). Given the three-state model for the "dimeric" mixed-valence complexes outlined above, a similar basis is formulated for the strong IR activity in symmetric pyrazine modes of $\mathbf{1}^{-}-\mathbf{4}^{-}$.

5. Multidimensional Potential Surfaces and Electronic Localization

With respect to vibronic signatures of bridging ligand vibrations in both IR and Raman spectra, the three-state model agrees well with experimental observations for $\mathbf{1}^{-}-\mathbf{4}^{-}$. However, at first glance the three-state model appears to assume a *delocalized* system that does not match the dynamic, *localized* electronic behavior of $\mathbf{1}^{-}-\mathbf{4}^{-}$ evident in their partially coalesced C−O stretching IR bands. Indeed, it has been asserted that a main drawback of the three-state model is its limitation to delocalized systems.[58] In reality, however, the only limitations of this model are to cases with large exchange coupling interactions between charge-site-based and bridge-based electronic states in which the transformation from three neighboring electronic basis states to three Hückel "molecular orbitals" is a reasonable one.

A defining way to investigate a model's prediction of electronic "localization" or "delocalization" is to look at the ground state potential energy surface predicted by the model. If the ground state potential surface exhibits two minima, then the complex is at least partially "localized" or valence-trapped and Robin−Day class II; if it only has one minimum, then the complex is "delocalized" or averaged-valence and Robin−Day class III. A significant realization of vibronic models is that they show that nuclear dynamics can still be very important even in formally "delocalized", single-minimum systems, and thus the distinction between "localized" and "delocalized" is more a semantic distinction than one that predicts radical differences in the behavior of complexes that are "localized" or "delocalized". The semiclassical Marcus−Hush model, which is formulated explicitly in terms of potential surfaces and assumes the Born−Oppenheimer approximation, predicts the limit for delocalization to be $\lambda \leq 2H_{AB}$, in which the electronic coupling, H_{AB}, has completely overcome the reorganization energy for ET, λ. The Ondrechen three-state model and the two-state PKS model do *not* assume the Born−Oppenheimer approximation, so it becomes more difficult to explicitly define a limit for localization or delocalization. A (somewhat artificial) application of the Born−Oppenheimer approximation to the vibronic models can generate potential surfaces that allow tentative conclusions about localization or delocalization to be made. Again, it is important to realize that in vibronic models, "delocalized" complexes can display important dependences on nuclear dynamics, and can themselves display a large range of behavior depending on their degree of delocalization, so the distinction between "localized" and "delocalized" is a more semantic than physical distinction.

For the most sophisticated presentations of the three-state model, which explicitly include vibronic coupling to bridge-based modes, the only Born−Oppenheimer surfaces that have been determined are for specific parametric limits that assume a delocalized system and yield only single-minimum ground-state surfaces.[41] However, in the simpler formulations of the model that do not explicitly couple bridge-based modes to the electronic problem,[35,37] double-minimum surfaces are easily generated. The delocalization limit for the simpler models is

$$\frac{A^2(U+\alpha)}{KU(U-\alpha)} < 1 \qquad (2)$$

where $U = \sqrt{\alpha^2+8J^2}$ and A is the vibronic coupling constant for the vibrations that are considered most important to the electron-transfer process, which are the charge-site breathing modes (in linear combinations q and Q) in the strict small-polaron formulation of the model. The general shape of the potential surfaces here is defined by the force constants of the important normal modes. In the case of $\mathbf{1}^{-}-\mathbf{4}^{-}$, the "B" surface is expected to be very flat and "soft" due to the low frequencies of both the symmetric cluster breathing modes and the cluster−bridging ligand stretching modes.

For $\mathbf{1}^{-}-\mathbf{4}^{-}$, complementary data and some important assumptions allow the estimation of parameters of the three-state model. The energy of the B → N transition is given in eq 1, and in the limit of large exchange coupling (J) this transition energy is expected to be dominated by J and only slightly modified by α.[59] If the energy of the B → N transition is taken to be 11 000 cm^{-1}, then J should be close to 4000 cm^{-1}. α can be estimated from the energy of two electronic transitions in "monomeric" cluster species: the transition from a core cluster level to the cluster antibonding level, and the transition from a core cluster level to a bound pyrazine ligand's π* level. The difference between these energies, which is approximately 4000−6000 cm^{-1}, should provide an estimate of the energy gap α between pyrazine and cluster levels. K for either cluster−bridging ligand stretching modes or symmetric cluster breathing modes can be determined from the frequency and normal-mode analyses in section 2.4. In the absence of quantitative low-frequency resonance Raman data, the most difficult parameter to estimate is the main vibronic coupling constant A to the modes that are most important to the ET process.[60] In a near-delocalized system, this vibronic coupling constant should be relatively small, because a greater dependence of the ET process on nuclear coordinates would lead to a more "localized" complex. This parameter is chosen arbitrarily to place the system close to the delocalization threshold, and it comes at the low end of the numerical region specified as typical of transition metal complexes by Ondrechen.[31] Across the series $\mathbf{1}^{-}-\mathbf{4}^{-}$, the main

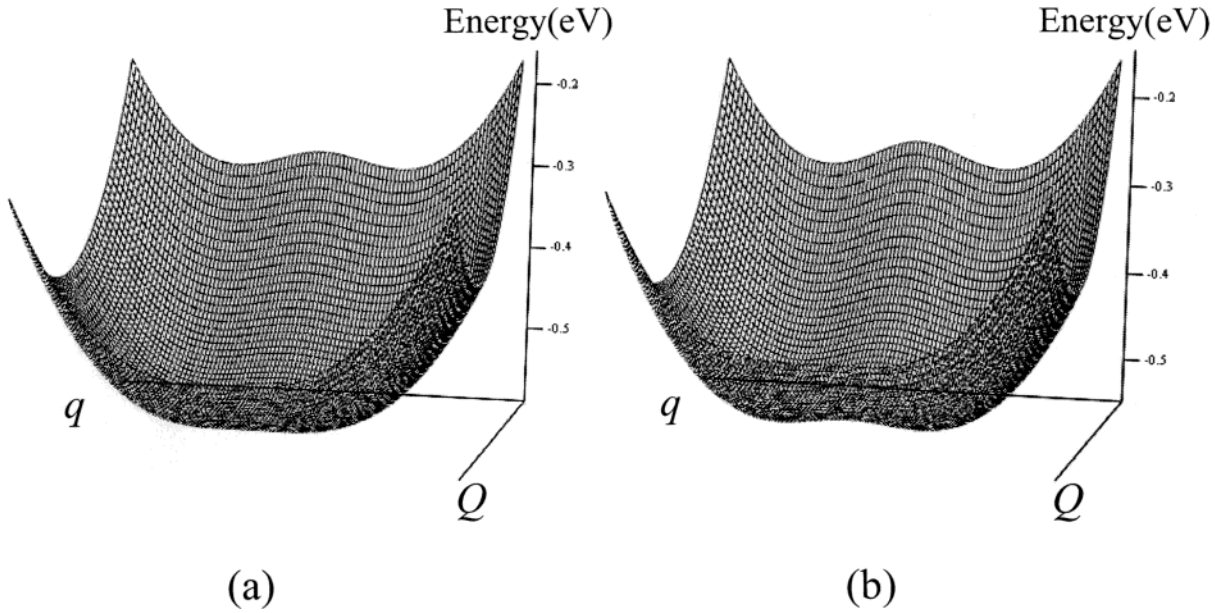

Figure 13. Representative "B" ground-state potential surfaces from the three-state model[37] close to the delocalization (single-minimum) limit with with parameters: (a) $J = -0.5$ eV, $A = 0.8$ eV/Å, $K = 1.0$ eV/Å^2, and $\alpha = 0.5$ eV; (b) $J = -0.5$ eV, $A = 0.8$ eV/Å, $K = 1.0$ eV/Å^2, and $\alpha = 0.7$ eV. Note that as α increases, the energy barrier between the two minima along q, the ET coordinate in this formulation, increases incrementally.

parametric variation is expected to be in α as described below, because all of these mixed-valence complexes are qualitatively identical and only differentiated by small orbital energy differences.

In $\mathbf{1}^-$−$\mathbf{4}^-$, if the π-acceptor effects of the ancillary pyridyl ligands L are neglected, then variation of L should have the main effect of changing α, the difference in energy between a cluster-based (−1) basis electronic state and the bridge-based (−1) basis electronic basis state. A better donor L ligand, like 4-(dimethylamino)pyridine in **1**, would lead to smaller α, whereas a weaker donor like 4-cyanopyridine in **4** would lead to an increased α.[61] In the simplest model which introduces α as an adjustable parameter,[37] variations in α of the order estimated from intrinsic reduction potentials of clusters with different ancillary ligands[12] can lead to small but important changes in the height of the thermal barrier to ET on a two-well "B" potential energy surface (see Figure 13). This control of the apparent thermal barrier to ET on the "B" surface via small synthetic adjustments in energy gap mirrors the trend observed in the electron-transfer rates apparent in the partially coalesced carbonyl IR bands of $\mathbf{1}^-$−$\mathbf{4}^-$,[3] and in principle it provides a simple, quantitative explanation for the unique "fine-tunability" of ET rates as probed by the carbonyl IR band shape in these complexes.

The lowest energy traces along the 2-dimensional potential surfaces of Figure 13 qualitatively resemble the one-dimensional potential surfaces that can be generated from Marcus−Hush theory, but there are fundamental and important differences between even a pseudo-one-dimensional trace and the Marcus−Hush treatment. In the Marcus−Hush model, the general picture (including the shape of the adiabatic potential surfaces) is defined by λ, the reorganization energy for electron transfer, and H_{AB}, the electronic coupling between only two electronic states; in the Ondrechen model, the model is framed in terms of specific molecular orbital overlap and normal-mode parameters. The vibronic model also includes non-Born−Oppenheimer effects, which are a natural consequence of ET-related mixing of vibronic states, and thus the extracted potential surfaces are only a piece of the full vibronic description. The semiclassical Marcus−Hush theory can easily be framed within transition state theory to predict thermal electron-transfer rates (which in the light of studies on $\mathbf{1}^-$−$\mathbf{4}^-$ appear to be nonphysical in the near-delocalized limit), whereas the vibronic three-state model can present a view that explicitly involves nuclear reorganization in a more direct molecular context that is perhaps more realistic in the near-delocalized limit.

Semiquantitatve ideas about the magnitude of the thermal barrier to ET on a two-well "B" potential surface can be generated in the three-state model, but quantitative calculation of thermal ET rates is not currently realistic because the surfaces have been extracted using the artifical assumption of the Born−Oppenheimer approximation in the context of a vibronic model. A more accurate calculation of ET rates in such a model would be to use time-dependent, wave packet techniques with significant non-Born−Oppenheimer adjustments to understand motion across the "B" surface. However, the experimental observation that ET rates in $\mathbf{1}^-$−$\mathbf{4}^-$ are strongly dependent on dynamic solvent dipolar relaxation suggests that motion across the "B" surface as presented in Figure 13 is probably not the limiting factor for the dynamic ET process. Rather, introduction of the solvent as either a frictional effect[62] or as its own, slower moving, orthogonal coordinate[63] are potential theoretical approaches to the necessary inclusion of dynamical solvent effects and prediction of thermal ET rates.[64]

Recent articles have shown that the Marcus−Hush model should be applicable at all magnitudes of electronic coupling up to the delocalized boundary for mixed-valence complexes.[65,66] However, both in the case of the Creutz−Taube ion and in $\mathbf{1}^-$−$\mathbf{4}^-$, a strong case can be made that such a model is not expected to be physically realistic due to both (1) the need for explicit inclusion of the bridging ligand in a full description of such complexes, and (2) significant non-Born−Oppenheimer effects introduced by vibronic coupling and the evident need of a vibronic model to account for the specific activity of molecular normal modes in electron transfer and delocalization.

6. Conclusions

The specific applicability of the Ondrechen three-state model to electron transfer in the ruthenium cluster mixed-valence

complexes $\mathbf{1}^{-}-\mathbf{4}^{-}$ is shown. The predictions of the model vis-a-vis vibronic signatures in symmetric bridging ligand modes have been realized in both resonance Raman and IR spectroscopy. Resonance Raman results show that the "intervalence" band of these complexes is better considered to be a B → N transition in the context of the delocalized molecular electronic states of the three-state model. Single-electron occupation of the Hückel-type three-state model means that it is not expected to need augmentation to higher, multielectron levels of theory in this particular case.

The specific normal modes most important to the dynamic, thermal ET process in $\mathbf{1}^{-}-\mathbf{4}^{-}$ are not currently experimentally available, but frequency calculations shed light on the *low* frequencies of important modes in these complexes and the probable thermal excitation of these modes at experimental temperatures. Given reasonable estimates of the specific model parameters for such Ru cluster mixed-valence complexes, the trend of slight adjustments in thermal ET rates via ancillary ligand substitutions is qualitatively reproduced in barrier heights on two-minimum Born−Oppenheimer potential surfaces generated from a simplified three-state model.

A general conclusion is that in bridged, strongly communicating mixed-valence systems such as $\mathbf{1}^{-}-\mathbf{4}^{-}$, a *vibronic* model that explicitly includes the participation of the bridging ligand is needed to fully account for the spectroscopic behavior. The phenomenon of partial infrared band coalescence due to fast ET rates allows dynamic interrogation of the specific complexes discussed here, but the conclusions made are expected to be general for near-delocalized mixed-valence systems.

7. Calculation Details and Experimental Methods

7.1. Density Functional Calculations. All density functional calculations were performed using Becke's three-parameter hybrid functional[67] and the exchange correlation of Lee, Yang, and Parr,[68] with the Los Alamos double-ζ quality basis set and effective core potentials,[69,70] or B3LYP/LANL2DZ, using Gaussian98[71] running on a single-processor PentiumIII linux workstation. This basis set/functional combination has been shown to reproduce metal carbonyl stretching frequencies to within 1% accuracy.[72] Geometry optimizations with MOs were generated for both the (0) and (−1) charge states (using restricted open-shell DFT) of the "monomeric" ruthenium complex to verify that the same cluster orbital is the (0) HOMO and (−1) LUMO. Frequencies are reported here for only the neutral species. Frequencies were computed using analytical second derivatives.

7.2. Infrared Spectroelectrochemistry. Solids of $\mathbf{1}^{-}-\mathbf{4}^{-}$ have proved difficult to isolate, due in part to their very negative reduction potentials[2,3] and resulting sensitivity to trace water and oxygen, so spectroelectrochemistry has been the main tool for in situ characterization. All infrared spectra (including those for **5**) were performed using a custom spectroelectrochemical cell[73] built in-house. Supporting electrolyte was 0.1 M tetrabutylammonium hexaflorophosphate in methylene chloride. Spectra reported here and in ref 5 were recorded at a temperature of −40 °C. The spectral window of these measurements was limited to $\nu > 1000$ cm^{-1} by the CaF_2 salt window; other materials were too brittle at similarly low temperatures to use in the "sandwich" design without damage.

7.3. Raman Spectroelectrochemistry. Raman spectra[6] were collected in the same spectroelectrochemical cell with the same electrolyte solution, aligned in a backscattering geometry and without temperature control (approximately room temperature). Low-frequency Raman spectra (<900 cm^{-1}) were difficult to interpret due to low signal and large low-frequency artifacts due to the solvent, electrolyte, and the spectroelectrochemical cell.

Acknowledgment. Funding from the National Science Foundation is acknowledged in support of this research (CHE-0079182 and CHE-0315593).

References and Notes

(1) Demadis, K. D.; Hartshorn, C. M.; Meyer, T. J. *Chem. Rev.* **2001**, *101*, 2655−2685.
(2) Ito, T.; Hamaguchi, T.; Nagino, H.; Yamaguchi, T.; Washington, J.; Kubiak, C. P. *Science* **1997**, *277*, 660−663.
(3) Ito, T.; Hamaguchi, T.; Nagino, H.; Yamaguchi, T.; Zavarine, I.; Richmond, T.; Washington, J.; Kubiak, C. P. *J. Am. Chem. Soc.* **1999**, *121*, 4625−4632.
(4) Londergan, C. H.; Salsman, J. C.; Ronco, S.; Dolkas, L. D.; Kubiak, C. P. *J. Am. Chem. Soc.* **2002**, *124*, 6236−6237.
(5) Londergan, C. H.; Salsman, J. C.; Ronco, S. R.; Kubiak, C. P. *Inorg. Chem.* **2003**, *42*, 926−928.
(6) Londergan, C. H.; Rocha, R.; Brown, M. G.; Kubiak, C. P.; Shreve, A. P. *J. Am. Chem. Soc.*, in press.
(7) Sutin, N. S. *Prog. Inorg. Chem.* **1983**, *30*, 441−498.
(8) Creutz, C.; Taube, H. *J. Am. Chem. Soc.* **1969**, *91*, 3988−3989.
(9) Hupp, J. T. The Creutz-Taube Ion: Electronic Structure of an Archetypal Mixed-Valence Complex. In *Comput. Coord. Chem. II*; Meyer, T. J., Ed.; Kluwer Academic Publishers: New York (in press).
(10) Petrov, V.; Hupp, J.T.; Mottley, C.; Mann, L. C. *J. Am. Chem. Soc.* **1994**, *116*, 2171−2172.
(11) Lu, H.; Petrov, V.; Hupp, J. T. *Chem. Phys. Lett.* **1995**, *235*, 521−527.
(12) Imai, N.; Yamaguchi, T.; Hamaguchi, T.; Ito, T.; Londergan, C. H.; Kubiak, C. P. Submitted for publication.
(13) Piepho, S. B.; Krausz, E. R.; Schatz, P. N. *J. Am. Chem. Soc.* **1978**, *100*, 2996−3005.
(14) Prassides, K.; Schatz, P. N. *J. Phys. Chem.* **1989**, *93*, 83−89.
(15) Wong, K. Y. *Inorg. Chem* **1984**, *23*, 1285−1290.
(16) Wong, K. Y.; Schatz, P. N. *Prog. Inorg. Chem.* **1981**, *28*, 369−449.
(17) Schatz, P. N.; Piepho, S. B.; Krausz, E. R. *Chem. Phys. Lett.* **1978**, *55*, 539−542.
(18) Krausz, E.; Burton, C.; Broomhead, J. *Inorg. Chem.* **1981**, *20*, 434−435.
(19) Painelli, A.; Girlando, A. *J. Chem. Phys.* **1986**, *84*, 5655−5671.
(20) Wong, K. Y.; Schatz, P. N. *Chem. Phys. Lett.* **1984**, *108*, 484−489.
(21) Anderson, G. R.; Devlin, J. P. *J. Phys. Chem.* **1975**, *79*, 1100−1102.
(22) Kral, K. *Czech J. Phys. B* **1976**, *26*, 660−669.
(23) Rice, M. J. *Phys. Rev. Lett.* **1976**, *37*, 36−39.
(24) Rice, M. J.; Lipari, N. O.; Strassler, S. *Phys. Rev. Lett.* **1977**, *39*, 1359−1362.
(25) Rice, M. J. *Solid State Commun.* **1979**, *31*, 93−98.
(26) Rice, M. J.; Yartsev, V. M.; Jacobsen, C. S. *Phys. Rev. B* **1980**, *21*, 3437−3446.
(27) Hush, N. S. *ACS Symp. Ser.* **1982**, *198*, 301−332.
(28) Simoni, E.; Reber, C.; Talaga, D. S.; Zink, J. I. *J. Phys. Chem.* **1993**, *97*, 12678−12684.
(29) Talaga, D. S.; Zink, J. I. *J. Phys. Chem.* **1996**, *100*, 8712−8721.
(30) Talaga, D. S.; Zink, J. I. *J. Phys. Chem. A* **2001**, *105*, 10511−10519.
(31) Ondrechen, M. J.; Ko, J.; Zhang, L.-T. *J. Am. Chem. Soc.* **1987**, *109*, 1672−1676.
(32) Ferretti, A.; Lami, A.; Ondrechen, M. J.; Villani, G. *J. Phys. Chem.* **1995**, *99*, 10484−10491.
(33) Ondrechen, M. J.; Ratner, M. A. *J. Chem. Phys.* **1977**, *68*, 938−946.
(34) Root, L. J.; Ondrechen, M. J. *Chem. Phys. Lett.* **1982**, *88*, 538−542.
(35) Root, L. J.; Ondrechen, M. J. *Chem. Phys. Lett.* **1982**, *93*, 421−424.
(36) Ondrechen, M. J.; Ko, J.; Root, L. J. *J. Phys. Chem.* **1984**, *88*, 5919−5923.
(37) Ko, J.; Ondrechen, M. J. *Chem. Phys. Lett.* **1984,** *112*, 507−512.
(38) Ko, J.; Ondrechen, M. J. *J. Am. Chem. Soc.* **1985**, *107*, 6161−6167.
(39) Ko, J.; Zhang, L.-T.; Ondrechen, M. J. *J. Am. Chem. Soc.* **1986**, *108*, 1712−1713.

(40) Zhang, L.-T.; Ko, J.; Ondrechen, M. J. *J. Am. Chem. Soc*. **1987**, *109*, 1666−1671.
(41) Zhang, L.-T.; Ko, J.; Ondrechen, M. J. *J. Phys. Chem.* **1989**, *93*, 3030−3034.
(42) Ondrechen, M. J.; Gozashti, S.; Zhang, L.-T.; Zhou, F. *Adv. Chem. Ser*. **1990**, *226*, 225.
(43) Zhang, L.-T.; Ondrechen, M. J. *Inorg. Chim. Acta* **1994**, *226*, 43−51.
(44) Ferretti, A.; Lami, A.; Ondrechen, M. J.; Villani, G. *J. Phys. Chem.* **1996**, *100*, 20174.
(45) Murga, L. F.; Ondrechen, M. J. *Theor. Chim. Acta* **1995**, *90*, 331−339.
(46) Cotton, F. A.; Norman, J. G., Jr. *Inorg. Chim. Acta* **1972**, *6*, 411−419.
(47) Baumann, J. A.; Salmon, D. J.; Wilson, S. T.; Meyer, T. J.; Hatfield, W. E. *Inorg. Chem.* **1978**, *17*, 3342−3350.
(48) Baumann, J. A.; J., S. D.; Wilson, S. T.; Meyer, T. J. *Inorg. Chem.* **1979**, *18*, 2472−2479.
(49) Robin, M.; Day, P. *Adv. Inorg. Chem. Radiochem.* **1967**, *10*, 247.
(50) Reimers, J. R.; Hush, N. S. *Chem. Phys.* **1996**, *208*, 177−193.
(51) Strekas, T. C.; Spiro, T. G. *Inorg. Chem.* **1976**, *15*, 974−975.
(52) The cluster breathing mode that best represents the bond-length adjustments made to a Ru trinuclear cluster upon electron transfer is expected to resemble the fully symmetric cluster breathing mode, but with opposite Ru−C(carbonyl) and Ru−N bond length changes. This ET-associated motion is expected to have a low frequency (but probably not quite as low) similar to that of the fully symmetric cluster breathing mode.
(53) It is *not* necessarily clear that asymmetric bridge vibrations should have a role similar to that of the asymmetric cluster breathing or cluster−bridging ligand stretching modes.
(54) Lord, R. C.; Marston, A. L.; Miller, F. A. *Spectrochim. Acta* **1957**, *9*, 113−125.
(55) Simmons, J. D.; Innes, K. K.; Begun, G. M. *J. Mol. Spectrosc.* **1964**, *14*, 190−197.
(56) Direct investigation of ν_{6a} ($\nu \approx 700$ cm^{-1} in **1**−**4**) has not been possible in either infrared or Raman spectroscopy due to specific experimental issues (see section 7).
(57) The near-infrared spectrum of the (−1) state of this "monomeric" cluster exhibits two overlapping bands that presumably have mixed cluster-to-ligand charge-transfer character and should be vibronically coupled to both symmetric cluster breathing modes and symmetric pyrazine breathing modes. Resonance Raman spectroscopy in these bands is expected to confirm vibronic coupling to symmetric pyrazine modes.
(58) Crutchley, R. J. *Adv. Inorg. Chem.* **1994**, *41*, 273−325.
(59) In the case of the Creutz−Taube ion, both α and *J* are determinable because there are two bands evident, the B → N and N → A transition, available due to ground-state electronic occupation in both the "B" and "N" levels of the model. Single electron occupation of the three-state model in $\mathbf{1}^{-}$−$\mathbf{4}^{-}$ presents the disadvantage of only one allowed electronic transition and requires α to be estimated from other measurements.
(60) Both cluster breathing and cluster−bridging ligand stetching modes should be important to the cluster-to-cluster ET process, and for best accuracy they should both be explicitly considered. The simplified model used in section 5 only includes a single intramolecular ET coordinated for graphical purposes.
(61) A minor effect of varying α in this way would be to also vary *J*, because a smaller difference in energy should lead to larger exchange coupling between adjacent electronic states. However, because *J* is so favorable in all of $\mathbf{1}^{-}$−$\mathbf{4}^{-}$ and because the favorable spatial overlap between cluster and bridging ligand orbitals is identical, it can be assumed that for small variations in α, the main influence of varying the ancillary ligand L is a changing α and adjustments to *J* can be overlooked.
(62) Tominaga, K.; Walker, G. C.; Kang, T. J.; Barbara, P. F. *J. Phys. Chem.* **1991**, *95*, 10485−10492.
(63) Sumi, H.; Marcus, R. A. *J. Chem. Phys.* **1986**, *84*, 4894−4914.
(64) It has been demonstrated in simulations[74] that Marcus−Hush potential surfaces with applied solvent friction cannot predict the fast ET rates observed by carbonyl infared band coalescence.
(65) Nelsen, S. F. *Chem. Eur. J.* **2000**, *6*, 581−588.
(66) Brunschwig, B. S.; Creutz, C.; Sutin, N. *Chem. Soc. Rev.* **2002**, *31*, 168-184.
(67) Becke, A. D. *J. Chem. Phys*. **1993**, *98*, 5648−5652.
(68) Lee, C.; Yang, W.; Parr, R. G. *Phys. Rev. B* **1988**, *37*, 785−789.
(69) Dunning, T. H., Jr.; Hay, P. J. In *Methods of Electronic Structure and Theory*; Schaefer, H. F., III., Eds.; Plenum Press: New York, 1977; Vol. 2.
(70) Hay, P. J.; Wadt, W. R. *J. Chem. Phys*. **1985**, *82*, 270−283.
(71) Frisch, M. J.; Trucks, G. W.; Schlegel, H. B.; Scuseria, G. E.; Robb, M. A.; Cheeseman, J. R.; Zakrzewski, V. G.; Montgomery, J. A., Jr.; Stratmann, R. E.; Burant, J. C.; Dapprich, S.; Millam, J. M.; Daniels, A. D.; Kudin, K. N.; Strain, M. C.; Farkas, O.; Tomasi, J.; Barone, V.; Cossi, M.; Cammi, R.; Mennucci, B.; Pomelli, C.; Adamo, C.; Clifford, S.; Ochterski, J.; Petersson, G. A.; Ayala, P. Y.; Cui, Q.; Morokuma, K.; Malick, D. K.; Rabuck, A. D.; Raghavachari, K.; Foresman, J. B.; Cioslowski, J.; Ortiz, J. V.; Stefanov, B. B.; Liu, G.; Liashenko, A.; Piskorz, P.; Komaromi, I.; Gomperts, R.; Martin, R. L.; Fox, D. J.; Keith, T.; Al-Laham, M. A.; Peng, C. Y.; Nanayakkara, A.; Gonzalez, C.; Challacombe, M.; Gill, P. M. W.; Johnson, B. G.; Chen, W.; Wong, M. W.; Andres, J. L.; Head-Gordon, M.; Replogle, E. S.; Pople, J. A. *Gaussian 98*, revision A.9; Gaussian, Inc.: Pittsburgh, PA, 1998.
(72) Zhou, M.; Andrews, L.; Bauschlicher, C. W. *Chem. Rev.* **2001**, *101*, 1931−1962.
(73) Zavarine, I. S.; Kubiak, C. P. *J. Electroanal. Chem.* **2001**, *495*, 106−109.
(74) Maroncelli, M. P. Personal communications.